Collective Effects in the $P^{31}(He^3,p)S^{33}$ Reaction*

R. S. Cox AND R. W. West
Department of Physics, University of Kansas, Lawrence, Kansas 66044

AND

R. J. Ascuitto
Department of Physics, University of Kansas, Lawrence, Kansas 66044
and
Lawrence Radiation Laboratory, Berkeley, California 94720

(Received 21 May 1968)

The two-nucleon transfer reaction has been used to study collective effects in the ground and first three excited states of S^{33} through the $P^{31}(He^3,p)S^{33}$ reaction at 6 MeV. The angular distribution of outgoing protons, measured in 5° intervals over the angular range from 0° to 75°, was analyzed in terms of the distorted-wave Born approximation and the strong-coupling collective model. Optical-model parameters were determined from measurements of the elastic scattering of He^3 by P^{31}. It was found that the shape of the angular distribution of reaction protons leading to the ground state of S^{33} is sensitive to the amount of d-wave admixture introduced into the $2s_{1/2}$ orbital by the deformation of the nucleus. It was found that the ground-state distribution could be reproduced with a deformation of -0.20, which compares well with the value of -0.17 determined from the quadrapole moment of S^{33}.

I. INTRODUCTION

THE S^{33} nucleus has now received the attention of a large number of investigators, and a full compilation of the information obtained as of 1967 is given by Endt and Van der Leun.[1] Briefly, the energy levels have been found primarily through the $S^{32}(d,p)S^{33}$ reaction and the l_n values determined for transitions to several excited states. Spin assignments have been made using the $S^{32}(d,p\gamma)S^{33}$ reaction[2,3] and the $S^{32}(n,\gamma)S^{33}$ reaction.[4] Theoretical calculations in terms of the collective model have been done by Bishop[5] and more recently by Malik[6] while shell-model work was carried out by Glaudemans, Wiechers, and Brussaard[7] and more recently by Bouten, Elliott, and Pullen[8] and by Glaudemans, Wildenthal, and McGrory.[9] Although the later work has shown much better agreement with the experimental level sequence than earlier work, it is clear that neither model can simply explain the level structure of the mass-33 system.

As is true for many nuclei, much of the useful information on S^{33} has been obtained by means of single-nucleon transfer reactions. However, two-nucleon transfer reactions can serve as a supplementary tool, in some cases providing information which is not available from single-nucleon transfer reactions. This observation is well illustrated in the present study of the $P^{31}(He^3,p)S^{33}$ reaction to the ground state which is especially sensitive to d-wave admixtures to the $2s_{1/2}$ pure shell-model orbital.

In the pure shell-model limit we note that the stripped proton enters the $2s_{1/2}$ orbital, whereas the stripped neutron enters the $d_{3/2}$ orbital, and an $L=2$ angular distribution is predicted for the outgoing proton. If we now think in terms of the collective model and allow the final product to take on a negative deformation (as might be suggested by the sign of its quadrupole moment, -0.64 b), the proton will enter the $\frac{1}{2}[211]$ orbital and the neutron the $\frac{3}{2}[202]$ orbital (see Fig. 1). The $\frac{3}{2}[202]$ orbital remains a pure d state, whereas, the collective potential introduces d-state components into the $\frac{1}{2}[211]$ orbital. An explanation of this $L=0$ admix-

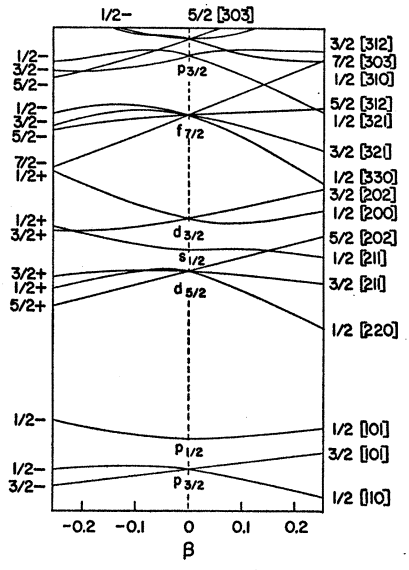

FIG. 1. Nilsson diagram.

* Supported in part by the U. S. Atomic Energy Commission.

[1] P. M. Endt and C. Van der Leun, Nucl. Phys. **A105**, 1 (1967).
[2] J. A. Becker, L. F. Chase, Jr., D. B. Fossan, and R. E. McDonald, Phys. Rev. **146**, 761 (1966).
[3] J. M. O'Dell, R. W. Krone, and F. W. Prosser, Jr., Nucl. Phys. **82**, 574 (1966).
[4] G. Van Middel Koop and H. Gruppel Laar, Nucl. Phys. **80**, 321 (1966).
[5] G. R. Bishop, Nucl. Phys. **14**, 376 (1959).
[6] F. B. Malik (private communication).
[7] P. W. M. Glaudemans, G. Wiecher, and P. J. Brussaard, Nucl. Phys. **56**, 529 (1964); **56**, 548 (1964).
[8] M. C. Bouten, J. P. Elliot, and J. A. Pullen, Nucl. Phys. **A97**, 113 (1967).
[9] P. W. M. Glaudemans, B. H. Wildenthal, and J. B. McGrory, Phys. Letters **21**, 427 (1966).

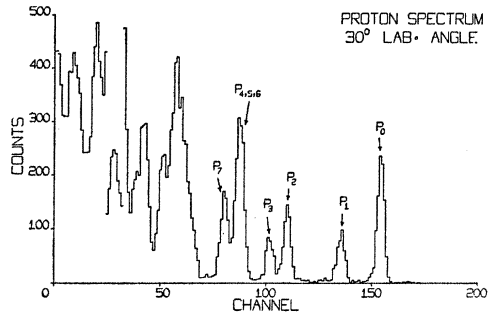

FIG. 2. Typical proton spectrum. Protons leaving S^{33} in its ground and first seven excited states are indicated.

ture can also be made in terms of the shell model when configuration mixing is included. However, the dominant configurations of the present shell-model wave functions[7] seem to rule out this possibility, and we shall continue this discussion in terms of the collective model.

If one were to look for the d-wave admixture in the $2s_{1/2}$ shell-model state with a single-nucleon transfer reaction, again a reaction leading to the occupation of this state would be used (e.g., $Si^{28}(d,p)Si^{29}$). In all such cases one would have to determine the $L=2$ admixture in a predominantly $L=0$ distribution, a situation in which the over-all shape of the angular distribution is relatively insensitive to the amount of the admixture. Hence one would expect the $P^{31}(He^3,p)S^{33}$ reaction to provide a measure of this admixture to an accuracy which cannot be as easily obtained from single-nucleon transfer reactions.

The present work was undertaken to study the $P^{31}(He^3,p)$ reaction leading to the low lying states of S^{33} and particularly to investigate the $L=0$ admixture to the ground-state distribution. The collective model was chosen in the interpretation of the results. In this model the amount of admixture can be easily associated with the nuclear-deformation parameter β, and thus a comparison of the value of β obtained here to the measured electric quadrupole moment provides a consistency test of the method of analysis.

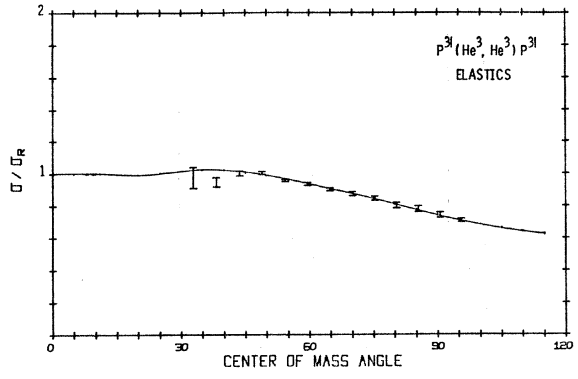

FIG. 3. Elastic scattering normalized to Rutherford scattering. The solid curve represents the optical-model fit for both sets I and II of optical-model parameters listed in Table I.

II. EXPERIMENTAL METHOD

A rough calculation shows that the height of the Coulomb barrier of P^{31} for He^3 ions is about 6.7 MeV. To enhance the yield, it is necessary to conduct the experiment at least close to, if not above, this energy. To obtain 6 MeV He^3 ions, the doubly-charged component of the University of Kansas' three-million-volt Van de Graaff beam was extracted by magnetic analysis and brought to the scattering chamber. Typical on-target currents were about 150 namp, which represented approximately 0.3% of the total current output of the rf ion source. The much more intense singly-charged component was used to regulate the terminal voltage.

Targets for use in measurements of the elastic cross section were made by evaporating a 20-$\mu g/cm^2$ layer of red phosphorous onto thin carbon backings. The phosphorous evaporation was immediately followed by a thin overlay of gold which prevented the loss of phosphorous during bombardment and also provided a high-Z element with a Coulombic elastic cross section. Instrumental effects could then be accounted for by comparing the angular dependence of the results for gold with Rutherford scattering. For the (He^3,p) measurements, targets were made by evaporating a 70-$\mu g/cm^2$ Zn_3P_2 layer onto gold backings again followed by a thin overlay of gold. The resulting targets were found to be more stable during the much longer runs at higher currents necessitated by the extremely low-reaction cross section.

Reaction protons were detected by a silicon surface-barrier detector mounted on the rotatable lid of the 6-in.-diam chamber with which the scattering angle could be determined to within $\frac{1}{2}°$. The detector was mounted so that scattered particles were incident at an oblique angle to its front face. With an effective thickness of about 1700 μ the highest-energy protons produced in the reaction were stopped in the active volume. To prevent radiation damage, particularly at small scattering angles, the proton counter was covered with a nickel foil just thick enough to remove 6-MeV He^3 ions, which permitted the measurement of outgoing protons through 0°. The zero angle of scattering was determined from the symmetry of the proton yield about 0° and was in agreement with the estimated accuracy of the mechanical beam-alignment procedures and the scale markings of the rotatable lid. The acceptance angle of the detector collimation was about 4°.

Relative cross sections were obtained by use of a fixed monitor counter positioned at 135° in which elastically scattered He^3 ions were observed. Normalization to absolute cross section was obtained from subsequent measurements of the angular distribution of elastically scattered He^3 ions and a determination of the yield ratio of reaction protons to the elastic group at an arbitrary angle. An important factor in the accuracy of the quoted absolute cross section is the assumption that the elastic cross section for angles less

TABLE I. Optical-model parameters.

He^3 Parameter set no.	V (MeV)	W (MeV)	r_0 (fm)	a_0 (fm)	r_0' (fm)	a_0' (fm)	r_c (fm)	
I	76.867	15.080	1.588	0.589	1.541	0.611	1.3	Present data
II	116.066	19.475	1.530	0.582	1.502	0.597	1.3	Present data
III	76.800	13.000	1.070	0.854	1.8	0.65	1.4	a
Proton								
IV	57.00	8.50	1.11	0.62	1.11	0.62	1.3	b

[a] Reference 2. [b] Reference 5.

than 45° is due solely to Coulomb scattering. This assumption is believed to be justified and will be discussed more fully in Sec. III.

Data were collected in 5° intervals over the angular range from 0° to 75° with several angles repeated to check for reproducibility. The output of the detectors was amplified and brought to the two halves of a 400-channel pulse-height analyzer. In this arrangement counting losses in the electronics reduced all yields by the same factor and thus, corrections for these errors were unnecessary. Figure 2 shows an example of the spectra obtained from the proton detector at a laboratory angle of 30°. Protons corresponding to the ground and first three excited states of S^{33} are clearly resolved. Other unresolved proton groups appearing in the lower channels are from higher states in S^{33} and contaminants in the target.

III. OPTICAL-MODEL PARAMETERS

The angular distribution of He^3 ions elastically scattered from P^{31} is shown in Fig. 3. The cross section has been normalized to the angular dependence of Rutherford scattering. The error bars indicate only the statistical accuracy of the data. As mentioned above, the elastic cross section was assumed to be equal to the Rutherford cross section for angles less than 45°. This assumption is believed to be justified for the following reasons:

(1) Since the incident He^3 energy is close to the Coulomb-barrier height, the cross section would be expected to approach Rutherford scattering at forward angles.

(2) The ratio of the elastic cross section from P^{31} to that of the Au approached a constant value at forward angles. Since the Au cross section may be assumed to be pure Coulomb scattering, this result eliminates the possibility that an accidental systematic error caused the P^{31} scattering to approach a constant value at forward angles.

(3) The present experimental results agree with measurements of elastic scattering for He^3 ions under similar experimental conditions. In particular, the report of Bray, Nurzynski, and Satchler[10] on the $Al^{27}(He^3,He^3)$ reaction at 5.5 MeV shows a deviation from Rutherford scattering of less than 3% for angles forward of 44°. Furthermore, the slow, smooth angular dependence of their yield showing a knee followed by an almost linear falloff toward increasing angles is the same as that observed in the present experiment. Similar angular dependences have been reported by Cline, Alford, and Blau[11] for the $Ca^{40}(He^3,He^3)$ reaction near 9 MeV and by Blau, Alford, Cline, and Gove[12] for the $K^{39}(He^3,He^3)$ reaction at 9 MeV.

Two sets of optical-model parameters for the He^3 projectile were obtained by fitting the elastic scattering. The potential considered was

$$U(r)=V_c(r,r_c)-VF(r,r_0,a)-iWF(r,r_0',a'),$$

where

$$F(r,r_0,a)=\{1+\exp[(r-r_0A^{1/3})/a]\}^{-1}.$$

V and W are the well depths for the real and imaginary parts of the optical-model potential, and V_c is the Coulomb potential from a uniformly charged sphere of radius $r_cA^{1/3}$. A is the mass number of the target, and the geometrical parameters are r_0, a_0, r_0', and a_0'.

The parameters were obtained by minimizing the normalized χ^2.

$$\chi^2=\frac{1}{N-k}\sum_{i=1}^{N}\left[\frac{\sigma_{\text{expt}}(\theta_i)-\sigma_{\text{theor}}(\theta_i)}{\Delta\sigma_{\text{expt}}(\theta_i)}\right]^2,$$

where N is the number of experimental points considered, k is the number of parameters, σ_{expt} and σ_{theoret} are the experimental and theoretical cross sections at the angle θ_i, and $\Delta\sigma_{\text{expt}}$ is the corresponding experimental error. Initial values of the parameters were taken from the work of Bray *et al.*[10] for 5.5-MeV He^3 ions on Al^{27}, and the work of Yntema, Zeidman, and Bassel[13] for 12-MeV He^3 ions on Ca^{40}. The resulting parameters are labeled in Table I as sets I and II, respectively. Set I resulted in a slightly smaller χ^2 and gave a better fit to the data at large angles; however, the differences in the fits are indistinguishable from the solid curve shown in

[10] K. H. Bray, J. Nurzynski, and G. R. Satchler, Nucl. Phys. **67**, 417 (1965).

[11] W. P. Alford, L. M. Blau, and D. Cline, Nucl. Phys. **73**, 33 (1965).

[12] L. M. Blau, W. P. Alford, D. Cline, and H. E. Gove, Nucl. Phys. **76**, 45 (1966).

[13] J. L. Yntema, B. Zeidman, and R. H. Bassel, Phys. Letters **11**, 302 (1964).

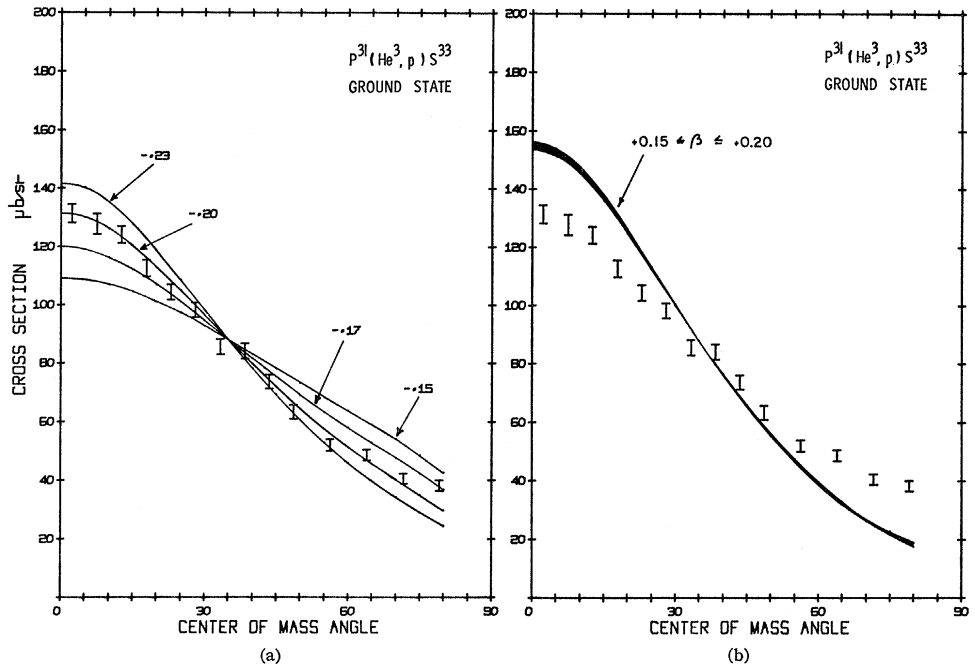

FIG. 4. Ground-state angular distribution. (a) Solid curves are the fits resulting for various negative values of the deformation parameter. The fits have been arbitrarily normalized at 35°. Set I of the optical-model parameters were used throughout. (b) Solid curve represents the fits resulting from positive deformations between +0.15 and +0.20. The fits were normalized at 35° and set I of optical-model parameters were used.

Fig. 3. The parameters obtained by Bray *et al.* for Al^{27} are reproduced in Table I as set III.

The last entries of Table I, set IV, are the optical-model parameters for the outgoing proton which were taken from the work of Cohen and Cookson[14] for elastic proton scattering from Si^{28} at 11.98 MeV.

IV. $P^{31}(He^3,p)S^{33}$ ANALYSIS

The experimental results were interpreted in terms of the two-nucleon stripping theory.[15,16] The target and final product of the reaction were described by the strong-coupling collective model. The basic assumption of this model is that the nucleus is composed of a permanently deformed core and a number of extra core nucleons. Since the potential field experienced by the extra core nucleons is due to the mass distribution of the core, it is assumed to possess the same symmetry as the core. If we assume that the collective coordinates do not change appreciably because of the reaction, then, in the limit of axial symmetry and noninteracting extra core nucleons, the target and final product may be described by a symmetrized-state function[17] of the form

$$\psi_{MK}{}^{I}=\left(\frac{2I+1}{16\pi^2(1+\delta_{\Omega_p,0}\delta_{\Omega_n,0})}\right)^{1/2}\phi_{\text{vib}}\times[D_{MK}{}^{I*}(\theta_i)\chi_{\Omega_p}(\rho_1,\cdots,\rho_{N_p})\chi_{\Omega_n}(\eta_1,\cdots,\eta_{N_n})+(-1)^{I-N_p/2-N_n/2}D_{M-K}{}^{I*}(\theta_i)\chi_{-\Omega_p}(\rho_1,\cdots,\rho_{N_p})\times\chi_{-\Omega_n}(\eta_1,\cdots,\eta_{N_n})],$$

where I, M, and K represent the total angular momentum, its projection on the laboratory z axis, and its projection on the nuclear symmetry axis, respectively. $D_{MK}{}^{I}$ is the rotation matrix[18] which describes the orientation of the system through the Euler angles θ_i; $\chi_{\Omega p}(\rho_i,\cdots,\rho_{Np})$ and $\chi_{\Omega n}(\eta_1,\cdots,\eta_{Nn})$ describe the shell structure and are normalized determinantal wave functions composed of N_p proton and N_n neutron deformed orbitals, respectively; and ϕ_{vib} is the zero-point vibration eigenfunction. The arguments ρ_i and η_i are the coordinates necessary to specify the ith proton and jth neutron with respect to the body-fixed axis system.

The condition of axial symmetry requires $K=\Omega_p+\Omega_n$ with

$$\Omega_p=\sum_{i=1}^{N_p}\Omega_i,$$

$$\Omega_n=\sum_{j=1}^{N_n}\Omega_j.$$

Each particle state is described by a deformed Nilsson orbital[19]

$$\chi_\Omega=\sum_j C_{j\Omega}\chi_{j\Omega},$$

where Ω is the projection of the particle's angular momentum (j) on the nuclear symmetry axis. The expansion coefficients for states of negative projection are given by

$$C_{j-\Omega}=(-1)^{1/2-j}C_{j\Omega}.$$

[14] A. V. Cohen and J. A. Cookson, Nucl. Phys. **24**, 529 (1961).
[15] H. C. Newns, Proc. Phys. Soc. (London) **A76**, 489 (1960).
[16] N. K. Glendenning, Phys. Rev. **137**, B102 (1965).
[17] A. Bohr, Kgl. Danske Videnskab. Selskab, Mat. Fys. Medd. **26**, 14 (1952).
[18] M. E. Rose, *Elementary Theory of Angular Momentum* (John Wiley & Sons, Inc., New York, 1957).
[19] S. G. Nilsson, Kgl. Danske Videnskab. Selskab, Mat. Fys. Medd. **29**, 16 (1955).

The corresponding angular distribution becomes[16]

$$\frac{d\sigma}{d\Omega}(i\rightarrow f)\propto\sum_{LSJ}\sum_{M_L}|R_{L_{if}}{}^{M_L}(\mathbf{k}_{He^3},\mathbf{k}_p)|^2,$$

where i and f specify the target and final product of the reaction. $R_{L_{if}}{}^{M_L}(\mathbf{k}_{He^3},\mathbf{k}_p)$ is the standard stripping integral familiar from single-nucleon transfer reactions.[20] In this case, the stripping integral contains the weighted bound-state wave function for the c.m. of the captured particles (1 and 2)

$$\phi_{LSJ}(\text{c.m.})=\sum_N A_{NLSJ}[I_fK_f;\Omega_1\Omega_2;I_iK_i],$$

where the sum is over the states (specified by N) necessary to describe the c.m. of the captured particles. Here the mixing amplitudes $A_{NLSJ}[I_f,K_f;\Omega_1,\Omega_2;I_i,K_i]$ become

$$\begin{aligned}&A_{NLSJ}[I_fK_f;\Omega_1\Omega_2;I_iK_i]\\&=\sum_n f_n(\beta_0\eta_p)\sum_{j_1j_2}\langle n0,NL,L|n_1l_1,n_2l_2,L\rangle\\&\times\Big\{\lambda\theta_{\text{vib}}(2I_i+1/2I_f+1)^{1/2}C_{j_1\Omega_1}C_{j_2\Omega_2}\\&\times C(j_1j_2J;\Omega_1\Omega_2\Omega)C(I_iJI_f;K_i\Omega K_f)\\&\times[(2j_1+1)(2j_2+1)(2L+1)(2S+1)]^{1/2}\\&\times\begin{Bmatrix}l_1&\frac{1}{2}&j_1\\l_2&\frac{1}{2}&j_2\\L&S&J\end{Bmatrix}\Big\},\end{aligned}$$

where n specifies the internal motion of the captured particles. In this expression mixing from different oscillator shells has been neglected. Also, the results for axial asymmetry follow directly when the amplitudes are summed over Ω_1 and Ω_2. Similar expressions can be derived for the capture of identical particles. If one assumes a Gaussian wave function for the incident He^3 projectile, then

$$\begin{aligned}f_n(\beta_0\eta_p)\propto&[\Gamma(n+\tfrac{3}{2})/\Gamma(n+1)]^{1/2}\\&\times(6\eta_p{}^2/\beta_0{}^2-1)^n/(6\eta_p{}^2/\beta_0{}^2+1)^{n+3/2},\end{aligned}$$

where Γ is the Γ function, β_0 is the inverse oscillator length and η_p is the projectile size parameter. $\langle no,NL,Ll\ n_1l_1,n_2l_2,L\rangle$ is the Moshinsky transformation bracket,[21] $C(j_ij_2j_3;m_1m_2m_3)$ is the Clebsch-Gordan coefficient,[18] and

$$\begin{Bmatrix}l_1&\frac{1}{2}&j_1\\l_2&\frac{1}{2}&j_2\\L&S&J\end{Bmatrix}$$

is a 9-J symbol.[18] The value of λ is $\sqrt{2}$ if either the target or final product is even-even; otherwise, λ is unity. θ_{vib} denotes the overlap between the vibration eigenfunction of the target and final product. This becomes unity for a perfect rotor. Additional selection rules are

$$\Omega=\Omega_1+\Omega_2,\quad j_1\geq|\Omega_1|$$
$$K_f=K_i+\Omega,\quad j_2\geq|\Omega_2|.$$

In this model, configuration mixing results from the nonspherical nature of the collective potential and is reflected in the angular distribution by the introduction of additional multipolarities not predicted by the pure shell model.

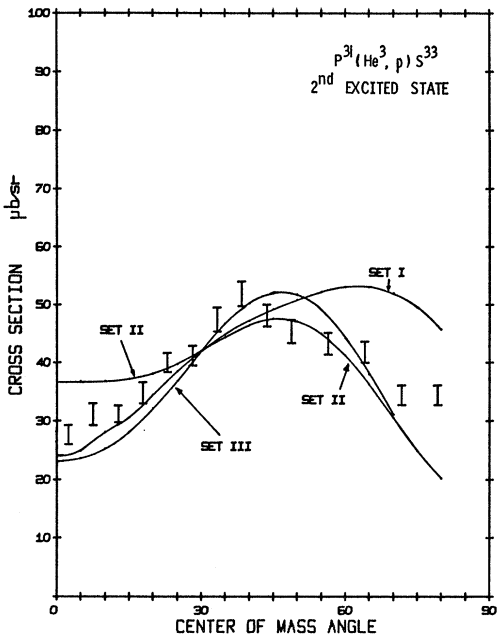

FIG. 5. Angular distribution for second excited state. The solid curves are the fits resulting from the three sets of optical-model parameters listed in Table I. The deformation was kept constant at −0.20. The fits were normalized at 30°.

V. INTERPRETATION OF EXPERIMENTAL RESULTS

The simplest model of S^{33} is the extreme single-particle model with pure Nilsson configurations. This means that the basic physical properties of S^{33} are attributed to a single neutron outside a deformed core. Also, any state of the nucleus is characterized by having the extra core neutron in a single Nilsson orbital. The problem of mixed Nilsson configurations will be discussed in the interpretation of the experiment.

The level sequence of S^{33} is $(\frac{3}{2}^+,\frac{1}{2}^+,\frac{5}{2}^+,\frac{3}{2}^+,\cdots)$. If one fills pairwise the Nilsson diagram in Fig. 1, then the only unfilled orbitals available to the odd neutron are $\frac{3}{2}[202]$ and $\frac{1}{2}[200]$. For a pure Nilsson configuration, the associated deformation parameter β[17] can be de-

[20] W. Tobocman, Phys. Rev. 94, 1655 (1954).
[21] T. A. Brody and M. Moshinsky, *Tables of Transformation Brackets* (Gordon and Breach Science Publishers, Inc., New York, 1967).

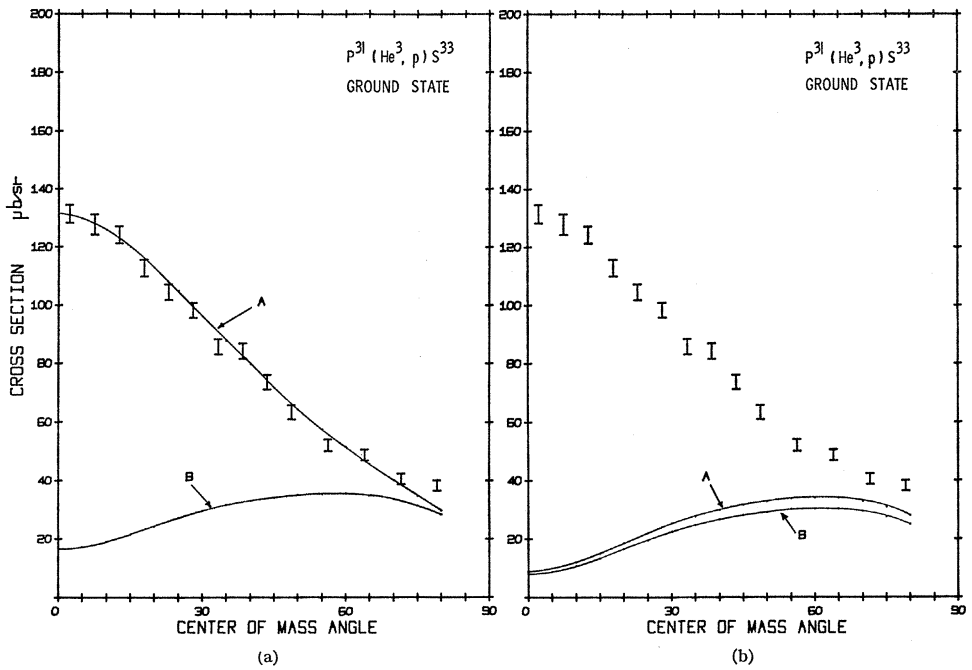

FIG. 6. (a) $d_{5/2}$ contribution to ground-state distribution. Curve A is the calculated cross section using optical set I and a deformation of -0.20. Curve B is the same cross section with all $d_{5/2}$ contributions removed. (b) $d_{5/2}$ contribution to $l=2$ part of ground-state distribution. Curve A is the $l=2$ part of the calculated cross section using optical set I and a deformation of -0.20. Curve B is the same cross section with all $d_{5/2}$ contributions removed.

termined from the quadrupole moment formula

$$Q\sim\frac{3Z}{(5\pi)^{1/2}}R_0\beta\left[\frac{3K^2-I(I+1)}{(I+1)(2I+3)}\right], \tag{1}$$

where R_0 is the nuclear radius. One assumes with this formula that the entire contribution to the quadrupole moment arises from the deformed core. It should be mentioned that if one considers mixed Nilsson configurations, this approximation may not be valid and the particle contributions should be included in Eq. (1). We mention this since, for mixed configurations, core states with different K can add both positively and negatively in the appropriate generalization of Eq. (1).

Let us consider first an interpretation of the ground and second excited state. For negative deformations, the ground state would consist of a neutron in orbital $\frac{3}{2}[202]$ which would establish a $K=\frac{3}{2}$ band head. The second excited state ($\frac{5}{2}^+$) would then be the first rotational member of this band. For this configuration, Eq. (1) yields a deformation of about -0.18. For positive deformations, a neutron would occupy the $\frac{1}{2}[200]$ orbital which would establish a $K=\frac{1}{2}$ band head. The decoupling parameter for the $\frac{1}{2}[200]$ orbital is such that an inverted-level sequence ($I=\frac{3}{2}$, $K=\frac{1}{2}$; $I=\frac{1}{2}$, $K=\frac{1}{2}$) may occur; however, other physical quantities, such as the moment of inertia of the S^{32} core, become unreasonable. For this configuration, however, the deformation parameter has the same magnitude as for the previous configuration but differs in sign.

We have analyzed the ground-state angular distribution for both of these configurations. In each case, the proton is assumed assimilated into the S^{32} core by occupying the $-\frac{1}{2}[211]$ orbital. Figure 4 shows the ground-state angular distribution for both positive and negative deformations using set I of the optical-model parameters. The best fit was obtained for a deformation of about -0.20. Sets II and III of the optical-model parameters agree with this value of the deformation.

Let us now examine how the properties of the individual capture orbitals are reflected in the angular distribution. In the deformed case, an $L=0$ admixture is introduced because of the configuration mixing in the $2s_{1/2}$ and $d_{3/2}$ orbitals; furthermore, the degree of the $L=0$ admixture is an implicit function of the nuclear-deformation parameter. One would also expect that this admixture would be favored because of the low energy of the incident projectile. For negative deformations, this admixture is a direct consequence of the $d_{3/2}$ and $d_{5/2}$ mixtures in the $-\frac{1}{2}[211]$ proton orbital, whereas for positive deformations the $L=0$ component is more pronounced because of the introduction of a $(2s_{1/2})^2$ configuration resulting from the $\frac{1}{2}[200]$ neutron orbital.

Let us now consider the second excited state because of its connection with the ground state. This level is assumed to be the first member of a rotational band built on the ground state. It therefore possesses the same shell structure and differs only in its rotational motion. For this level both $L=2$ and $L=4$ components are predicted; however, the $L=4$ component is very small. Figure 5 shows the angular distribution for the second excited state and the fits corresponding to all sets of optical-model parameters. The deformation was kept at -0.20.

A point that should be mentioned is that, since the $L=4$ admixture was very small, the shape of this distribution was quite insensitive to the nuclear deformation. Therefore, simple shapes of this type may be

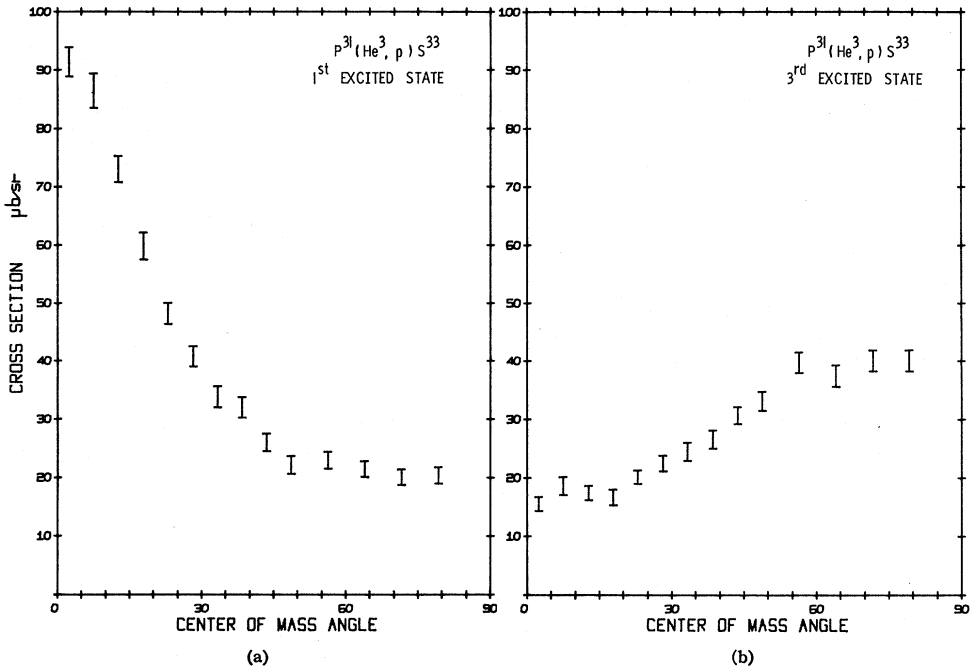

FIG. 7. (a) Experimental angular distribution for outgoing protons leaving S^{33} in its first excited state. (b) Experimental distribution for outgoing protons leaving S^{33} in its third excited state.

used as a guide for judging optical-model parameters. Also, optical-model parameters which gave a reasonable description of the shape for this level give a correspondingly good description of the shape for the ground state.

Glaudemans, Wiecher, and Brussaard[7] considered a shell model with configuration mixing for nuclei in the $2s_{1/2}$-$d_{3/2}$ shell. They allowed the particles all possible configurations in these shells with the Si^{28} core held inert. The dominant configurations for the ground states of P^{31} and S^{33} are given below:

$$\psi(P^{31})=0.8216\psi[s^3(\tfrac{1}{2},\tfrac{1}{2})]-0.5367\psi[s(\tfrac{1}{2},\tfrac{1}{2}),d^2(0,1)],$$

$$\psi(S^{33})=0.7880\psi[s^4(0,0),d(\tfrac{3}{2},\tfrac{1}{2})]-0.4000\psi[s^2(0,1),d^3(\tfrac{3}{2},\tfrac{1}{2})]-0.3564\psi[s^2(0,1),d^3(\tfrac{3}{2},\tfrac{3}{2})],$$

where the numbers in parentheses (J,T) represent the total angular momentum and isospin of either the $s_{1/2}{}^n$ or $d_{3/2}{}^m$ configuration. For this model, the preference is for the ground-state distribution to proceed by an $(s_{1/2},d_{3/2})$ configuration of the captured particles and hence multipolarity $L=2$. On the other hand, the present experiment shows that the $d_{5/2}$ admixtures for the Nilsson-configuration proton $-\frac{1}{2}[211]$ and neutron $\frac{3}{2}[202]$ in S^{33} are quite important. This is illustrated in Fig. 6(a), which shows a comparison of the ground-state distribution with the distribution which results when the $d_{5/2}$ contributions of the Nilsson-expansion coefficients are subtracted from the amplitudes $A_{NLSJ}[I_fK_f;\Omega_1\Omega_2;I_iK_i]$.

Figure 6(b) shows the corresponding change in the $L=2$ part of this distribution. As can be seen, the $d_{5/2}$ components are producing the large $L=0$ admixture for this configuration. The results shown here were obtained with a deformation of -0.20 and set I of the optical-model parameters, but the same general results held for the other sets of optical-model parameters.

While the qualitative shape of the ground and second excited state angular distributions are reproduced rather well with the model, we should mention that neither the absolute nor relative magnitude of the cross section was predicted with a high degree of accuracy. For example, the calculated relative yield of the ground and second excited states differs by a factor of 2.5 from the experimental result. Thus, in all the comparisons between experiment and theory, the theoretical curves have been arbitrarily normalized to the experimental data.

While part of the problem of reproducing the yields lies in the simplified model used here, the sensitivity of the yield to the optical-model parameters should not be overlooked. The elastic scattering data is dominated by Coulomb scattering at forward angles and data were not taken at backward angles where nuclear scattering is relatively larger. Both these facts tend to make a precise determination of the optical-model parameters difficult.

We turn now to a discussion of the first and third excited states of S^{33}. The nature of these states has been investigated by Bishop,[5] who showed that a simple lifting of the extra core neutron from the $\frac{3}{2}[202]$ orbital to the $\frac{1}{2}[200]$ orbital to establish the first excited state must be ruled out from excitation-energy considerations. His analysis also showed that a pure neutron-hole excitation to establish the first excited state (i.e., lifting

one of the two neutrons in the $\frac{1}{2}[211]$ orbital to pair off with the extra core $\frac{3}{2}[202]$ neutron) with the third excited state as a rotational band member gave the correct energy separation of these states with reasonable values of the collective model parameters.

A detailed calculation of the angular distribution to these states has not been attempted in the present work, however, some qualitative information can be gained from the amplitudes $A_{NLSJ}[I_fK_f;\Omega_1\Omega_2;I_iK_i]$. The experimental data for these two states are shown in Fig. 7. Unfortunately, a configuration based on a neutron-hole excitation cannot contribute to the reaction amplitude of the present model, and we can therefore not comment on the possibility of this mode of excitation. However, the amplitudes for a first excited state configuration based upon both captured particles entering the $\frac{3}{2}[202]$ orbital coupled to $\Omega=0$ are consistent with the observed forward peaking of the first excited state and the lack of forward peaking in the third excited state angular distributions. Finally, the negative results of Bishop for an excited state based upon the lifting of the extra core neutron are supported here by the fact that the amplitudes for a third excited state as a rotational band member of this configuration predict a forward-peaked angular distribution, contrary to the observed results.

ACKNOWLEDGMENT

We would sincerely like to thank Norman K. Glendenning for the use of his distorted-wave computer code for double stripping.

PHYSICAL REVIEW VOLUME 175, NUMBER 4 20 NOVEMBER 1968

Positron Decays of ^{38}Ca and ^{38}K

R. W. KAVANAGH
Institut de Recherches Nucléaires, Strasbourg, France and California Institute of Technology, Pasadena, California 91109

AND

A. GALLMANN, E. ASLANIDES, F. JUNDT, AND E. JACOBS*
Institut de Recherches Nucléaires, Strasbourg, France

(Received 13 May 1968)

The positron decay of ^{38}Ca has been investigated using the ^{36}Ar(^{3}He,n) reaction with an enriched ^{36}Ar gas target. A delayed 1568-keV γ ray with a half-life of 0.47±0.02 sec is attributed to a positron branch to the 1695-keV level of ^{38}K. Upper limits of 3% or better were found for transitions to other low-lying levels. Using the measured half-life and the decay energies, the branching ratio to the 1695-keV level is calculated from β-decay systematics to be (21±4)%. The logft for this transition (3.41±0.09) establishes $J^\pi=1^+$ for the 1695-keV level. An additional result was the observation of an allowed transition from ^{38}K to the 3936-keV level of ^{38}Ar.

I. INTRODUCTION

THE isotope ^{38}Ca has a mass 6736±27 keV greater than ^{38}K, and must therefore decay by superallowed β^+ emission to its isobaric analog level ($J^\pi=0^+$, $T=1$) at an excitation of 127 keV in ^{38}K.[1] The only reported evidence relating to this decay has been that of Cline and Chagnon,[2] who irradiated Ca and CaH_2 targets with 85-MeV bremsstrahlung and attributed a delayed γ ray, with energy 3.5±0.1 MeV and half-life 0.66±0.05 sec, to the reaction ^{40}Ca(γ,2n)^{38}Ca($\beta^+\gamma$)^{38}K. The assignment was based in part on the good agreement between the observed half-life and an earlier semiempirical estimate of 0.7 sec.[3] Using current, more accurate values for the total decay energy, $W_0=6098$ ±28 keV, and for the comparative half-life for such 0^+-to-0^+ transitions, $ft=3100\pm30$ sec,[4] one finds the corresponding partial half-life for ^{38}Ca to be 0.593 ±0.015 sec, also reasonably close to the observed value.

In view, however, of the systematic presence[5] of strong Gamow-Teller transitions in the $A=4N+2$ series of nuclei up to ^{30}P, the present work was undertaken to search for γ rays following β^+ transitions from ^{38}Ca to $J^\pi=1^+$ states of ^{38}K. One such was indeed found leading with a calculated relative intensity of 21±4%, to the known 1.7-MeV level of ^{38}K, and its half-life was measured to be 0.47±0.02 sec, in disagreement with the observation of Cline and Chagnon.

In the course of this work, a previously unreported transition from 7.68-min ^{38}K to the fourth excited state of ^{38}Ar was also observed.

* Research Fellow of the "Interuniversitair Institut voor Kernwetenschappen," Belgium. Permanent address: I.N W. Proeftuinstraat, Gent, Belgium.

[1] P. M. Endt and C. Van der Leun, Nucl. Phys. **A105**, 1 (1967).
[2] J. E. Cline and P. R. Chagnon, Phys. Rev. **108**, 1495 (1957).
[3] O. Kofoed-Hansen, Phys. Rev. **92**, 1075 (1953).
[4] J. N. Bahcall, Nucl. Phys. **75**, 10 (1966).
[5] R. W. Kavanagh (to be published).